Quickest Detection Framework for Signal Integrity Monitoring in Low-Cost GNSS Receivers

Daniel Egea-Roca, Gonzalo Seco-Granados, José A. López-Salcedo
Department of Telecommunications and Systems Engineering
Universitat Autònoma de Barcelona (UAB)
Bellaterra 08193, Barcelona (Spain)

***Abstract*—Recently, there has been an increasing interest in GNSS-based safety and liability applications. These applications, which are often associated to urban environments or in general to vehicular applications, have very stringent requirements in terms of accuracy, continuity and integrity of the provided position solution. In this paper, we present simple quickest threat detectors for being used in low-cost GNSS receivers. The aim is to detect the presence of interference and multipath as soon as posible in order to improve GNSS integrity.**

I. Introduction

In the past decade, Global Navigation Satellites Systems (GNSS) have played a prominent role in the development of urban navigation applications and new location-based services (LBS) [1]. The constant growth of these applications and services has been accompanied by an increase of requirements in terms of accuracy, continuity and more importantly, integrity of the position solution. In this context, *integrity* refers to the ability of the user receiver to guarantee the quality and trust of the received signal, in such a way that critical or commercial applications can be safely operated.

Recently, a plethora of vehicular GNSS-based applications have appeared involving safety of life features, such as the system for avoiding pedestrian traffic accidents proposed in [2], or involving liability critical applications like automatic road user charging or pay-per-use insurance [3], [4]. In these applications, it is of paramount importance to promptly detect any possible anomaly or misleading behaviour that could affect the received GNSS signal. Otherwise, we could be endangering the safety and trust of the end-user, thus causing a major trouble.

In the past years, different contributions for providing GNSS integrity have appeared. Most of them propose the use of external information like map-matching for identifying local threats (e.g. known interference sources or signal blocking obstacles) [5], external sensors for obtaining redundant information [6], or fisheye cameras to obtain a sky plot and determine the geometrical distribution of satellites in view [7]. Nevertheless, the use of external aid needs prior information about the user environment or external hardware, which is not always available in mass-market GNSS receivers (i.e. those mostly used for vehicular applications).

Apart from the above considerations, traditional GNSS integrity algorithms are not capable of providing an accurate and reliable position solution in urban environments (i.e. those where vehicular applications are mainly present), due to local effects like multipath, Non-Line-Of-Sight (NLOS) propagation and radio frequency interference. While significant research efforts have been devoted to the detection of these threats, most of the existing techniques still rely on classical detection schemes. This means that their performance metrics are typically in the form of probability of detection and false alarm, thus disregarding the temporal dimension (i.e. time-to-detect), which is indeed of paramount importance for integrity applications. It is for this reason that we propose the adoption of the so-called quickest detection framework, which targets the minimisation of the detection delay while guaranteeing a certain detection performance [8].

Hence, the distinctive point of our contribution is twofold: (i) we provide a quickest detection approach, which will exclude wrong measurements from the positioning calculation quicker than classical ones; (ii) we provide an additional level of integrity dealing with local effects (i.e. signal level integrity) without using any external aid. We already addressed this problem for the case of multi-antenna GNSS receivers in [9] and [10], and for single-antenna receivers in [8]. In this paper, though, we focus instead on low-cost single-antenna GNSS receivers such as those used in smartphones, which have low computational capabilities and are presenting an increase of use for vehicular applications. In these cases, it may be difficult to compute the metrics proposed in [8] due to the low computational capability of the receivers, and then simple metrics are needed.

The rest of this paper is organised as follows. Section II introduces the signal model and Section III presents the quickest detectors for interference and multipath, presenting numerical results to show the performance of the proposed detection techniques. Finally, Section IV concludes the paper.

II. Signal Model

Let us consider a sequence of K observations $\mathbf{x} \doteq [x(0), x(1), \ldots, x(v), \ldots, x(K-1)]^T$, where v is the time instant at which an integrity threat appears (i.e. unknown change time). Consequently, it is assumed that before v (i.e. at hypothesis $\mathcal{H}_0$) the observation $x(n)$ follows a given statistical distribution, whereas after the change (i.e. at hypothesis $\mathcal{H}_1$) it follows a different one:

$$\begin{aligned} \mathcal{H}_0 &: x(n) \sim f_0(x(n)), \quad n < v \\ \mathcal{H}_1 &: x(n) \sim f_1(x(n)), \quad n \geq v \end{aligned} \tag{1}$$

This work was partly supported by the grant TEC2014-53656-R.

Based on these premises, quickest detection aims at finding the strategy that minimises the detection delay (i.e. $\overline{\tau}$), while keeping the mean time between false alarms (i.e. $\overline{T}$) larger than a conveniently set value. For this purpose, the CUSUM algorithm was proposed, which is based on a very important concept in statistics, namely the logarithm of the likelihood ratio:

$$\mathrm{LLR}(n) \doteq \ln \frac{f_1(x)}{f_0(x)} \tag{2}$$

and referred to as the log-likelihood ratio (LLR). For the sake of clarity we have omitted the time index n from the independent random variables x, keeping in mind that each variable x corresponds to a given time instant (i.e. $x(n)$).

The CUSUM algorithm is an efficient statistical change detection algorithm defined as the following decision rule:

$$g(n) = \left(g(n-1) + \mathrm{LLR}(n)\right)^+ \geq h \tag{3}$$

with $g(0) = 0$ and $(x)^+ = \max(0, x)$. It is known that the CUSUM minimises $\overline{\tau}$ among all detection algorithms that satisfy $\overline{T} \geqslant N_{\mathrm{fa}}$, with the following optimal results that allows us to find the threshold h that guarantees a given false alarm rate N_{fa} [8]:

$$\begin{array}{rcl} \overline{T} & \geq & e^h = N_{\mathrm{fa}} \\ \overline{\tau} & \leq & \frac{h}{\mathrm{K}(f1,f0)} \end{array} \tag{4}$$

where $\mathrm{K}(f_1, f_0) \doteq \mathrm{E}_1\left[\mathrm{LLR}(n)\right]$ is the Kullback divergence.

III. Quickest Detection of Local Threats

This section describes the application of the CUSUM algorithm to GNSS integrity monitoring. To do so, we use the CUSUM algorithm for interference and multipath detection, which are two of the most relevant and common threats in urban GNSS environments. We show two simple metrics to be used in low computational capabilities receivers. These metrics are the estimation of the received power, for interference detection, and the code discriminator output (DLL) for multipath detection. The main difference between these metics and those proposed in [8] is the simplicity of the ones with respect to the others. This is so, because the estimation of the received power can be calculated easily from the received samples (i.e. squared modulus). In contrast to the kurtosis calculation, which needs the computation of the 4-th central moment, and then is more computational expensive. On the other hand, for the multipath metric in [8] we need a multi-correlator receiver, which is not often the case of low-cost receivers, in contrast to the DLL, which is implemented in any GNSS receiver.

A. CASE 1: Quickest interference detection

This section proposes a quickest detection framework for detecting interferences in GNSS, based on the detection of a change in the power of the received signal. We know that in the absence of interference (i.e. under $\mathcal{H}_0$), the received signal will be dominated by noise, since the GNSS signal remains under the noise floor, whereas in the presence of interference (i.e. under $\mathcal{H}_1$), the received signal will be dominated by the interference. Then the detection principle is based on the fact that in the absence of interference, the estimated power should be around the noise power within the corresponding bandwidth. On the other hand, in the presence of some interference, the estimated power should significantly deviate from that noise power.

Based on the above considerations, let us define the estimated receiver power $\hat{P}_r(m)$ at snapshot m as follows

$$\hat{P}_r(m) \doteq \frac{1}{N} \sum_{i=1}^{N} \left\| r\left(i + mN - N\right) \right\|^2 \tag{5}$$

with each snapshot including N samples of the received signal $r(n)$. It can be easily probed that in absence of interference $\|r(n)\|^2$ follows a central χ^2 distribution with two degrees of freedom. On the other hand, in the presence of interference it follows a non-central χ^2 with two degrees of freedom and non-central parameter related to the interference power. Therefore, if we define the metric based on the received power estimation as follows

$$x_r(m) \doteq \frac{\hat{P}_r(m)}{2\sigma_w^2} \tag{6}$$

with σ_w^2 the noise power (which may be estimated), we will obtain that the metric equals to one in the absence of interference, and it departs form one otherwise. This metric, by the central limit theorem, can be modelled as a Gaussian distribution with mean and variance related by the noise and interference power. Hence, as the statistical distribution of this metric is completely defined, we will be able to use the CUSUM algorithm as a Gaussian mean and variance change detector.

Now, we can use the central limit theorem (CLT) to approximate the statistical distribution of $x_r(m)$ as a Gaussian distribution. The CLT stands that the sum of N i.i.d. random variables with finite mean and variance approaches a Gaussian distribution when N is large enough. Therefore, we can write the following hypotheses:

$$\begin{array}{l} \mathcal{H}_0 : x_r(m) \sim \mathcal{N}\left(\mu_0^{(r)}, \sigma_0^{2^{(r)}}\right), \quad m < v \\ \mathcal{H}_1 : x_r(m) \sim \mathcal{N}\left(\mu_1^{(r)}, \sigma_1^{2^{(r)}}\right), \quad m \geq v \end{array} \tag{7}$$

with expressions for the mean and variance derived from the CLT as follows:

$$\begin{aligned} \mu_0^{(r)} &= \frac{\sigma_w^2}{2\sigma_w^2} \cdot \mathrm{E}\left[\chi_2^2\right] = 1 \\ \sigma_0^{2^{(r)}} &= \frac{1}{N}\left(\frac{\sigma_w^2}{2\sigma_w^2}\right)^2 \cdot \mathrm{var}\left[\chi_2^2\right] = \frac{1}{N} \\ \mu_1^{(r)} &= \frac{\sigma_w^2}{2\sigma_w^2} \cdot \mathrm{E}\left[\chi_2^2(\lambda)\right] = (1 + \mathrm{INR}) \\ \sigma_1^{2^{(r)}} &= \frac{1}{N}\left(\frac{\sigma_w^2}{2\sigma_w^2}\right)^2 \cdot \mathrm{var}\left[\chi_2^2(\lambda)\right] = \frac{1}{N}\left(1 + 2\mathrm{INR}\right) \end{aligned} \tag{8}$$

with INR the interference-to-noise ratio and $\lambda = 2 \cdot \mathrm{INR}$ the non-central parameter.

This is shown in Fig. 1, where the distribution of the proposed metric is shown for the cases of absence and presence of

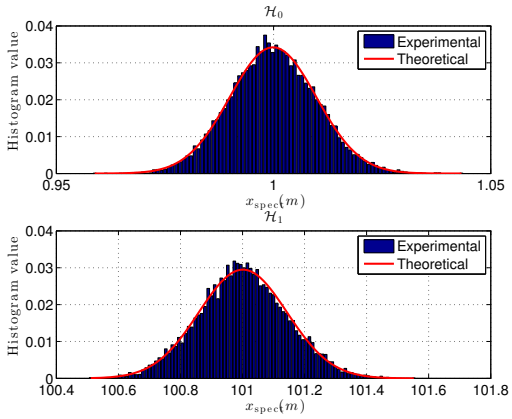

Fig. 1: Statistical characterisation for the power-based detection. Comparison between simulated (i.e. histogram) and theoretical PDF under $\mathcal{H}_0$ (up) and $\mathcal{H}_1$ (down).

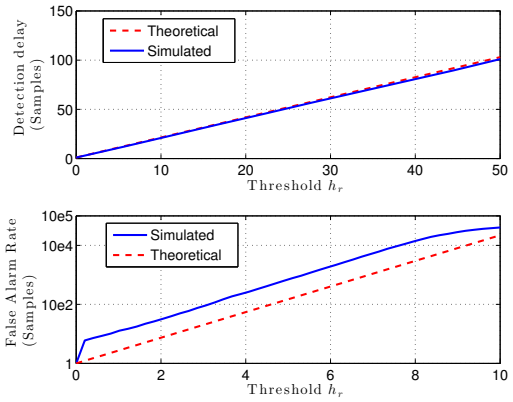

Fig. 2: CUSUM performance for the power-based method as a function of detection threshold. Detection delay for a CW with INR = -20dB (up) and false alarm rate in samples (down).

interference. We have used a noise power $\sigma_w^2 = 2$, $N = 1e4$, 1e5 Monte-Carlo runs and for the interference case we have simulated a continuous wave (CW) with INR = 20dB. We can notice the Gaussian distribution for both hypotheses. On the other hand, we can see the departure between the mean and variance under $\mathcal{H}_0$ (i.e. upper plot) and $\mathcal{H}_1$ (i.e. lower plot). Indeed, the mean under $\mathcal{H}_0$ should be close to one, whereas for the interference case the mean should be around the sum between the noise and interference power (see (8)).

From (7) we have statistically characterised the power estimate metric. This characterisation includes the mean and variance before and after the change, which are completely known from (8). Therefore, using the power estimation metric (i.e. $x_r(m)$), we can fully characterise the log-likelihood ratio, and then use the CUSUM algorithm for detecting both changes in the mean and variance. This gives rise to the following LLR:

$$\begin{aligned}\text{LLR}_r(m) = \ln\left(\frac{\sigma_0^{(r)}}{\sigma_1^{(r)}}\right) + \frac{\left(x_r(m)-\mu_0^{(r)}\right)^2}{2\sigma_0^{2(r)}} \\ - \frac{\left(x_r(m)-\mu_1^{(r)}\right)^2}{2\sigma_1^{2(r)}}.\end{aligned} \tag{9}$$

Both variance and mean after change depend on the INR of the interference. Thus, as in the interference case in [8], a way to proceed is to fix a certain value for these parameters according to the minimum INR that one expects to detect. Thereby, a minimum change detection is fixed allowing the detection of any larger change caused by larger INR. Hence, we can make use of the CUSUM algorithm as follows

$$g^{(r)}(m) = \left(g^{(r)}(m-1) + \text{LLR}_r(m)\right)^+ \geq h_{\text{r}} \tag{10}$$

leading to the following performance in terms of time between false alarms and detection delay

$$\begin{aligned}\overline{T}_r &\geq e^{h_r} \\ \overline{\tau}_r &\leq \frac{h_r}{\text{K}_r(f_1,f_0)}\end{aligned} \tag{11}$$

with $\text{K}_r(f_1,f_0) = \ln\left(\frac{\sigma_0^{(r)}}{\sigma_1^{(r)}}\right) + \frac{\left(\mu_1^{(r)}-\mu_0^{(r)}\right)^2}{2\sigma_0^{2(r)}}$.

These bounds are presented in Fig. 2 and compared with simulated results. To do so, we use $\sigma_w^2 = 2$, $N = 1e4$ and 1e5 Monte-Carlo runs. In addition, for the detection delay case we fix INR = -20dB. This low value is selected in order to show representative results, otherwise the detection delay would be one sample. The lower plot shows higher experimental samples between false alarms than the lower bound in (11). Therefore, the lower bound for the false alarm rate allows us to set a threshold h_r assuring certain desired false alarm rate. In addition, the upper plot shows similar values for the simulated results and theoretical ones.

Finally, it is worth to note that in this case $\text{K}_r(f_1,f_0) \approx 0.5$, whereas for the kurtosis metric proposed in [8] we would obtain $\text{K}_{\text{kurt}}(f_1,f_0) \approx 2.6\text{e-}11$ (i.e. calculating the kurtosis parameters with the simulation parameters used here). Hence, the interference metric proposed in this work outperforms the kurtosis metric proposed in [8] in terms of detection delay. However, in order to use the metric proposed here (i.e. $x_r(m)$) we must estimate the noise power previously, and then we are subject to the precision of the noise power estimator. Nevertheless, if we have a good estimation of the noise power, we will be able to eventually detect Gaussian wide-band interferences, which cannot be detected by the kurtosis metric because they will provide the same kurtosis as in the absence of interference (i.e. they are Gaussian).

B. CASE 2: Quickest multipath detection

Here, we present an application of quickest detection for detecting multipath in GNSS. The problem of multipath detection must be carried out at the acquisition and/or tracking stage, where measurements such as the estimated C/N_0, the code discriminator output (i.e. DLL) and the shape of the correlation curve fluctuates with the presence of NLOS and multipath [1]. Next, we show the application of the CUSUM algorithm for the DLL, which is a measurement available at the tracking loop of any GNSS receiver.

We know that under benign conditions (i.e. $\mathcal{H}_0$), the DLL is close to zero, with all variations due to the noise and to the small corrections needed to track the code dynamics (i.e. user movement). However, when a single multipath ray is present (i.e. $\mathcal{H}_1$) we see how the DLL output presents a spike in order to compensate the shift in the code position due to multipath. Afterwards, the DLL reverts to zero. Nevertheless, as the multipath conditions varies in practice, the DLL output will present different spikes along the period when multipath is present, which is translated to an increase of the variance of the DLL. Therefore, this is equivalent to a change on the DLL variance.

The DLL is calculated making use of the early and late correlators, which can be assumed to be Gaussian distributed since they are obtained from averaging Gaussian variables (i.e. correlators), and then we can formulate the problem of quickest multipath detection as follows:

$$\begin{aligned} \mathcal{H}_0 &: x_{\mathrm{d}}(k) \sim \mathcal{N}\left(\mu_0^{(\mathrm{d})}, \sigma_0^{2^{(\mathrm{d})}}\right), \quad k < v \\ \mathcal{H}_1 &: x_{\mathrm{d}}(k) \sim \mathcal{N}\left(\mu_0^{(\mathrm{d})}, \sigma_1^{2^{(\mathrm{d})}}\right), \quad k \geq v \end{aligned} \tag{12}$$

This is shown in Fig. 3, which shows the histogram of the DLL output values for data captured with a real GNSS receiver under the framework of the Integrity GNSS Receiver (iGNSSrx) project, funded by the European Commission. These data were gathered during 80 s by a moving vehicle in a dense urban environment, in London's (UK) downtown. The vehicle was under benign condition the first 40 s, and then it changed to harsh conditions until the end of the data record. We discriminate between benign and harsh conditions with the aid of a truth reference for calculating the position error. For the data under benign conditions we obtain a mean positioning error of 2m, whereas for the data under harsh conditions we obtain a mean positioning error of 50m. In the upper plot of Fig. 3 we present the histogram under benign conditions, where we see the Gaussianity of the DLL output with a mean close to 0 and low variance corresponding to variations of 0.015 chips (i.e. 1e-5) due to the noise and code dynamics. On the other hand, in the lower plot, we present the histogram under harsh conditions. We see how the histogram fits a Gaussian distribution too. In this case, the mean still is close to 0, but a much greater variance than under $\mathcal{H}_0$. The presented results correspond to one of the satellites in view. This is so in order to clarify the explanation, but the Gaussianity of the DLL output is maintained for all the satellites in view, and then the following discussion is valid regardeless of the tested satellite.

Hence, we see that the DLL follows a Gaussian distribution with known mean before and after change (i.e. 0) but unknown a priori variance before and after the change. Then, in order to use the CUSUM algorithm we propose the following configuration:

- $\mu_0^{(\mathrm{d})}$: We can fix it to 0 or calibrate it:

$$\mu_0^{(\mathrm{d})} = \kappa \approx 0 \tag{13}$$

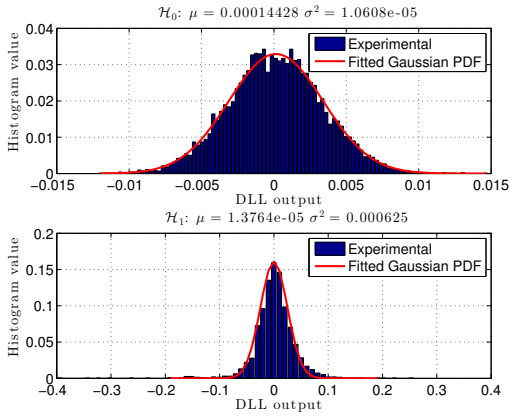

Fig. 3: Statistical characterisation of DLL output with real data captured in London downtown under benign conditions (up) and under harsh conditions (down).

- $\sigma_0^{2^{(\mathrm{d})}}$: This value is unknown a priori because it's difficult to have perfect knowledge of the actual variance, even knowing the expression for the variance of the DLL. This is so because it ultimately will depend on the multipath parameters, which will be random and unknown. Hence, we propose to fix the variance under benign conditions according to the maximum allowable variations on the DLL values under $\mathcal{H}_0$, as follows:

$$\sigma_0^{2^{(\mathrm{d})}} \doteq \left(\frac{(\Delta_0)_{\max}}{3}\right)^2 \tag{14}$$

  with $(\Delta_0)_{\max}$ the maximum allowable variations under $\mathcal{H}_0$. This is so because we know that for a Gaussian distribution the 99.86% of the values are comprised in the interval $\mu \pm 3\sigma$. For example, in our case we see that the DLL under $\mathcal{H}_0$ takes variations of ± 0.01 chips, which for GPS are equivalent to variations of $\pm$3m on the estimated pseudo-range. Thus, a proper consideration for the variations of the DLL output under $\mathcal{H}_0$ might be [3-10]m, and then larger variations are considered to be due to the presence of multipath. With this consideration, the DLL variation is between 0.01 and 0.034 chips, and then we may fix the maximum allowable variations to $(\Delta_0)_{\max} = 0.04$ chips. Doing so we obtain a variance before the change equal to $\sigma_0^{2^{(\mathrm{d})}} = 1.78\text{e-}4$.
- $\sigma_1^{2^{(\mathrm{d})}}$: Similarly as for the variance before change, we fix the variance under harsh conditions as the minimum detectable variability on the DLL due to multipath as follows:

$$\sigma_1^{2^{(\mathrm{d})}} \doteq \left(\frac{(\Delta_1)_{\min}}{3}\right)^2 \tag{15}$$

  with $(\Delta_1)_{\min}$ the minimum detectable variation on the DLL under $\mathcal{H}_1$. For instance, in our case, a suitable value might be a variation equivalent to ± 0.07 chips (i.e. 20m), which results in $\sigma_1^{2^{(\mathrm{d})}} = 5.5\text{e-}4$.

Therefore, with this configuration we are able to use the CUSUM algorithm for a Gaussian variance change, which has

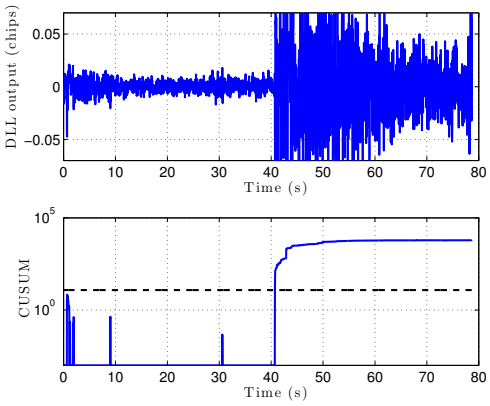

Fig. 4: Statistical characterisation of DLL with real data captured in London downtown under benign conditions (up) and under harsh conditions (down).

the following LLR:

$$\mathrm{LLR_d}(k) = \ln\left(\frac{\sigma_0^{(\mathrm{d})}}{\sigma_1^{(\mathrm{d})}}\right) + \frac{\left(x_\mathrm{d}(k) - \mu_0^{(\mathrm{d})}\right)^2 \left(\sigma_1^{2^{(\mathrm{d})}} - \sigma_0^{2^{(\mathrm{d})}}\right)}{2\sigma_0^{2^{(\mathrm{d})}}\sigma_1^{2^{(\mathrm{d})}}} \tag{16}$$

with $\mu_0^{(\mathrm{d})}$, $\sigma_0^{(\mathrm{d})}$, $\sigma_1^{(\mathrm{d})}$ defined as in (13)-(15), and $x_\mathrm{d}(k)$ the DLL output at the k-th post-correlation snapshot. Thereby, we can use the following decision rule:

$$g^{(\mathrm{d})}(k) = \left(g^{(\mathrm{d})}(k-1) + \mathrm{LLR_d}(k)\right)^+ \geq h_\mathrm{d} \tag{17}$$

leading to the next performance

$$\begin{array}{rcl} \overline{T}_\mathrm{d} & \geq & e^{h_\mathrm{d}} \\ \overline{\tau}_\mathrm{d} & \leq & \frac{h_\mathrm{d}}{\mathrm{K_d}(f_1,f_0)} \end{array} \tag{18}$$

with $\mathrm{K_d}(f_1,f_0) = \ln\left(\frac{\sigma_0^{(\mathrm{d})}}{\sigma_1^{(\mathrm{d})}}\right) + \frac{\sigma_1^{2^{(\mathrm{d})}}}{\sigma_0^{2^{(\mathrm{d})}}}$.

Here, we show the obtained DLL and the CUSUM evolution for the real data analysed in Fig. 3. This is shown in Fig. 4, where we see in the upper plot how the DLL presents a change in the variance just when multipath appears (i.e. second 40). This is promptly detected by the CUSUM, as it is shown in the lower plot, which shows how the CUSUM remains close to 0 (except some spikes due to the code dynamics) until it starts drifting upward at second 40 and it crosses the threshold. The threshold is set to fix a false alarm rate of 1h, which with a sampling rate of 10MHz and snapshot time of 20ms becomes equal to $h_\mathrm{d} = 12$ (black dashed line).

Finally, it is worth to mention that in this case we only need the early and late correlators for computing the DLL output, which are available on all GNSS receivers. On the other hand, for the SAM metric proposed in [8] we need the whole correlation curve (i.e. at least 5 correlation points), which are not available in all GNSS receivers (i.e. only the multi-correlators GNSS receivers). Hence, the multipath metric suggested here does not require a specific GNSS receiver and outperforms in terms of computation time the metric proposed in [8]. However, as a drawback, the suggested metric here is not able to discriminate between LOS and NLOS conditions, in contrast to the SAM metric. Nevertheless, for integrity monitoring we de not need to discriminate between these conditions, what is important is to detect the presence of multipath, which as we have shown is posible with the DLL.

IV. Conclusion

This paper presents a quickest detection framework for threat detection with the aim of improving integrity in GNSS, in order to be applied in emergent vehicular applications. Two different cases have been presented: quickest interference detection and multipath detection, both validated with simulated results and real measurements gathered by a vehicle in a urban environment, respectively. For the interference detection, we deal with a completely known LLR, whereas for multipath detection we deal with an incompletely known LLR (i.e. unknown variance), and both situations can be handled by the CUSUM algorithm. We proposed two methods that have been shown to outperform previous quickest detectors for interference and multipath in GNSS in terms of real-time capability. Moreover, the interference detection method provides a faster detection than previous approaches. This is so because the proposed metric is more sensible to interferences than other metrics, and then for the same interference power it presents a larger change. However, in order to calculate the metric proposed here we have to estimate the noise power. On the other hand, the multipath detection method can be applied to any GNSS receiver because it does not need any high-end or additional feature. Results of the proposed approaches show their suitability to be used in applications involving GNSS signal integrity real-time monitoring (i.e. safety of life and liability critical vehicular applications).

References

[1] G. Seco-Granados, J. A. López-Salcedo *et al.*, "Challenges in Indoor Global Navigation Satellite Systems: Unveiling its core features in signal processing," *IEEE Sig. Process. Mag.*, vol. 29, no. 2, pp. 108–131, 2012.

[2] X. Wu *et al.*, "Cars Talk to Phones: A DSRC Based Vehicle-Pedestrian Safety System," in *IEEE 80th VTC Fall*, 2014, pp. 1–7.

[3] J. Numrich, S. Ruja, and S. Voß, "Global Navigation Satellite System based tolling: state-of-the-art," *NETNOMICS: Economic Research and Electronic Networking*, vol. 13, no. 2, pp. 93–123, 2012.

[4] D. Salós *et al.*, "Analysis of GNSS integrity requirements for road user charging applications," in *Satellite Navigation Technologies and European Workshop on GNSS Signals and Signal Processing (NAVITEC), 2010 5th ESA Workshop on*, 2010, pp. 1–8.

[5] R. Toledo-Moreo *et al.*, "An analysis of positioning and map-matching issues for GNSS-based road user charging," in *Intelligent Transportation Systems (ITSC), 13th International IEEE Conference*, 2010.

[6] U. I. Bhatti and W. Y. Ochieng, "Detecting multiple failures in GPS/INS integrated system: a novel architecture for integrity monitoring," *Journal of Global Positioning Systems*, vol. 8, no. 1, pp. 26–42, 2009.

[7] E. Shytermeja, A. Garcia-Pena, and O. Julien, "Proposed architecture for integrity monitoring of a GNSS/MEMS system with a Fisheye camera in urban environment," in *ICL-GNSS*, 2014, pp. 1–6.

[8] D. Egea-Roca, G. Seco-Granados, and J. A. López-Salcedo, "On the Use of Quickest Detection Theory for Signal Integrity Monitoring in Single-Antenna GNSS Receivers," in *ICL-GNSS*, 2015, pp. 1–6.

[9] D. Egea *et al.*, "Interference and multipath sequential tests for signal integrity in multi-antenna GNSS receivers," in *IEEE 8th Sensor Array and Multichanel Signal Processing Workshop*, 2014, pp. 117–120.

[10] D. Egea, G. Seco-Granados, and J. A. López-Salcedo, "Single- and Multi-Correlator Sequential Tests for Signal Integrity in Multi-Antenna GNSS Receivers," in *ICL-GNSS*, 2014, pp. 117–120.